International Journal of Advance Research in Science and Engineering
Vol. No.6, Issue No. 03 , March 2017
www.ijarse.com
IJARSE
ISSN (O) 2319 - 8354
ISSN (P) 2319 - 8346

NUMERICAL SIMULATION OF SUPERSONIC FLOW PAST A BI-CONIC NOSE CONE

Piyush Kumar Pandey[1] , Bhavna Rajput[2],

Ashish Narayan[3], S.Narayanan[4]

[1,2]Post Graduate Student, [3]Research Scholar, [4]Assistant Professor,

Department of Mechanical Engineering, IIT(ISM) Dhanbad, (India)

ABSTRACT

The high-speed flow past a bi-conic nose cone is numerically investigatedin this paper. The primary focus of this paper is tooptimizethe parameters of bi-conic nose cone for augmenting the drag reduction. The bi-conic nose cones of different semi cone anglesat a cone base ratio (CBR) of 0.5 are studied in detail to determine the combination of parameters for minimum drag. The Mach no. contour represent the formation of bow shock after increasing the first semi cone angle from 40^o to 60^o. The pressure coefficient decreases rapidly up to a first cone angle of 40^o thereafter it shows a sudden increase followed by a decreasing behaviour. It is perceived that aerodynamic drag increases as we increase the semi cone angle at a fixed cone base ratio.

Keywords: Aerodynamics, Bi-Conic Nose Cone, Drag Reduction, Re-Entry Vehicle and Supersonic Flow

Nomenclature:L=total length of nosecone, L_1=length of first nose cone, L_2=length of second nose cone, R_1=Base radius of first cone, R_2= Base ratio of second cone, CBR= cone base ratio (R_1/R_2). ϕ_1=semi cone angle of first cone, ϕ_2=semi cone angle of second cone, ρ=density, u_x= axial velocity, u_r= radial velocity, p=pressure, E=total energy, M=Mach number, μ_t=Turbulent viscosity.

I. INTRODUCTION

Nose cones of different shapes are primarily used on the missile traveling at supersonic speed and are generally chosen with reference to combined aerodynamic, guidance and structural considerations. The bi-conic shape is one of the most appropriate alternatives to the standard nose cone. In particular, the bi-conic shapes are feasible in nature and versatile in design and give freedom to alter the geometrical configuration with specific properties. The bi-cone can be bluff bi-cone, slender bi-cone and bent bi-cone but here all the simulationsare done on simple sharp bi-cone. The bi-conic nose cone is applicable for a mission where a large cross-range capability, good flexibility, less retardation load and less landing distortion etc. Even through several studies on flow past a conic nose cones at supersonic Mach number are available but the detailed numerical studies of bi-conic nose cones for different parameters on the aerodynamics characteristics such as drag is scarce, which forms the specific objective of the present study. Due to the unavailability of many literatures on supersonic flow past bi-conic nose cones, some of the relevant literatures on conic and bi-conic nose cones are given below:

International Journal of Advance Research in Science and Engineering
Vol. No.6, Issue No. 03 , March 2017
www.ijarse.com
IJARSE
ISSN (O) 2319 - 8354
ISSN (P) 2319 - 8346

Arai, Sakaguchi [1] numerically investigated the separated flow around a bent-nose bi-conic. He captures the viscous effect on the body surface and no turbulence model is used. He confirmed that the separation around a bent-nose bi-conic is very similar to the open separation.

Anderson [2] gave a theoretical design study on characteristic study of a bi-cone mixed compression inlet for Mach 1.8 to 2.5. He found that the effect of increasing supersonic area contraction occurring internally from about 40 to 43 percent by decreasing the design second cone angle.

Richards et al [3] experimentally investigated the heat transfer and pressure distribution on sharp and finite bluntness and bi-conic geometries at various angle of attack in Mach 15-20 flow. He observed that the boundary layer thickness on these surfaces at high incidence to the flow was negligibly small. The shock shapes on bi-conic model at incidence indicated that the flow on the windward side of the model was subsonic even though the shock remained attached at the nose.

Claus Weiland [4] has described the aero-thermodynamic data of non-winged Re-entry vehicle (RV-NV).

II OBJECTIVE

Thefocusof this paper is to optimize the parameters of bi-conic nose conesfor minimum drag.The prominent parameters, which influences the aerodynamic characteristics,are first semi cone angle, second semi cone angle and cone base ratio. The paper also provide physical insight of the flow/shock features near the cone surface, which are expected toplay a significant role in controlling the drag reduction characteristics. Further, it provides the geometric optimization of the bi-conic nose cones for achieving minimum drag in supersonic vehicles.

III DESIGN PROCEDURE FOR THE BI-CONIC NOSE CONE MODEL

A bi-conic nosecone shape is simply a cone stacked on top of a frustum of a cone (commonly known to modellers as a 'conical transition section' shape), where the base of the upper cone is equal in diameter to the smaller diameter of the frustum. The sketch of the bi-conic nose cone shape of this current simulation has shown in Fig. 1. The following technique given below is adopted in the present study for the outline of various bi-conic nose cone models for increasing the drag reduction performance-

For $0 \le x \le L_1$

$$y = \frac{xR_1}{L_1}, \quad \dots (1)$$

$$\phi_1 = \tan^{-1}\frac{R_1}{L_1}, \quad \dots (3)$$

$$y = x \tan \phi_1, \quad \dots (5)$$

for $L_1 \le x \le L_2$

$$y = R_1 + \frac{(x - L1)(R_2 - R_1)}{L_1}, \quad \dots (2)$$

$$\phi_2 = \tan^{-1}\frac{R_2 - R_1}{L_1}, \quad \dots (4)$$

$$y = R_1 + (x - L_1)\tan \phi_2, \quad \dots (6)$$

IV. GOVERNING EQUATIONS

$$\frac{1}{r}\frac{\partial(\rho r u_r)}{\partial r} + \frac{\partial(\rho u_x)}{\partial x} = 0 \quad \dots (7)$$

$$\frac{1}{r}\frac{\partial(\rho r u_r u_r)}{\partial r} + \frac{\partial(\rho u_x u_r)}{\partial x} = -\frac{\partial p}{\partial r} + \frac{1}{r}\frac{\partial}{\partial x}\left[r\mu\left(\frac{\partial u_r}{\partial x} + \frac{\partial u_x}{\partial r}\right)\right] + \frac{1}{r}\frac{\partial}{\partial r}\left[r\,\mu\left(2\frac{\partial u_r}{\partial x} - \frac{2}{3}(\vec{\nabla}.\vec{u})\right] - 2\mu\frac{u_r}{r^2} + \frac{2}{3}\frac{u_r}{r}(\vec{\nabla}.\vec{u}) + \rho\frac{u_x^2}{r}, \quad \dots (8)$$

$$\frac{\partial(\rho u_x u_x)}{\partial x} + \frac{1}{r}\frac{\partial(\rho r u_x u_r)}{\partial r} = -\frac{\partial p}{\partial x} + \frac{1}{r}\frac{\partial}{\partial x}\left[r\mu\left(2\frac{\partial u_x}{\partial x} - \frac{2}{3}(\vec{\nabla}.\vec{u})\right] + \frac{1}{r}\frac{\partial}{\partial r}\left[r\mu\left(\frac{\partial u_r}{\partial x} + \frac{\partial u_x}{\partial r}\right)\right]\right. \quad \dots (9)$$

IJARSE
ISSN (O) 2319 - 8354
ISSN (P) 2319 - 8346

$$\nabla . E_t v = \rho f . v - \nabla . q - \nabla p . v \quad \ldots (10)$$

V SOLUTION METHOD

5.1 Computational Domain, Boundary Condition

The computational domain is fixed to 96R in axial and 48R in radial direction. The axisymmetric simulation is carried out with an implicit density based solver. No slip condition is applied at wall and fluid is considered as compressible ideal gas. The aerodynamic effects encounter in a flow field changes when gas no longer acts as a continuous medium and molecular characteristic of the gas become important. In the present study the law of continuum has been applied and hence the molecular ionization, dissociation and vibration are not considered because our primary focus is to investigate aerodynamics characteristic of the supersonic flow past over bi-conic nose cone.

5.2 Grid Independence Test

It is well known that the mesh quality (Fig.1) plays an important role in the accuracy level of the numerical results. Three different no. of cells were executed 140000, 155000 and 175000. The variation of Mach number and static pressure with position along the axis for various grids is shown in Fig. 4 for a CBR and semi-cone angle of 0.5 and 60^o. After comparison it is found that 155000 and 175000 grids did not result in significant change, hence the grid number 155000 cells are chosen as the grid independence solution for subsequent solution was carefully set to achieve a y+ value greater than 30.

VI. TURBULENCE MODEL

Spalart-Allmaras turbulent model is used in the current simulation. It is a one-equation turbulence model that has been developed mainly for aerodynamic application involving wall bounded flows and has been shown to give good results for boundary layers subjected to adverse pressure gradients. It is basically a transport equation. The dependent variable in this model is the eddy viscosity, whichis related directly to Reynold stress.

VII. VALIDATION

7.1 Comparison of Shock Angle Obtained From the Current Prediction with the Theory

In current computational study of high speed flow past over bi-conic nose cone when the supersonic flow past over bi-conic nose cone the first part of the shape behave as a single cone and the aerodynamic properties will be same as flow past over a cone, so we can compare the shock angle of bi-conic shape to the sharp cone. The shock angle is obtained for the various cone angle 5^o, 20^o, 40^o and 60^o is compared with the shock angle obtained by applet is given in table (1). William J. Davenport, department of aerospace and ocean engineering, Virginia Tech. designs the applet, Named as compressible aerodynamic calculator. There is another applet Shock-sim version 1.3e developed by NASA glen educational applets.

IJARSE
ISSN (O) 2319 - 8354
ISSN (P) 2319 - 8346

VIII RESULTS AND DISCUSSIONS

8.1 Variation of Mach Number And Static Pressure With Position Along The Axis Of Bi-Conic Nose Cone.

The variation of Mach no. and static pressure along the axis of a bi-conic nose cone for cone base-ratio (R_1/R_2) 0.5 for different value of both semi cone angle ϕ_1 (5^o, 20^o, 40^o, 60^o) & ϕ_2 (2.5^o, 10^o, 20^o, 30^o) is shown in Fig. 2 &Fig. 3. The attached shock is formed at ϕ_1= 5^o,20^o,40^o, but when the semi cone angle ϕ_1= 60^o the sudden jump occurs at some distance before the leading edge which give the indication of formation of bow shock (i.e., detached shock) and the distance between the leading edge and bow shock formed is called shock detachment distance.

8.2 Variation Of Pressure Coefficient Along The Bi-Cone Surface For Different Semi-Cone Angles And Constant CBR

The variation of pressure coefficient along the surface of bi-conic nose cone for CBR 0.5 at different semi-cone angles is shown in Fig.4. It can be seen from the graph that when we increase the semi cone angle the pressure coefficient decreases very fast and when ϕ_1=60^o at starting of second cone it increases first this is (due to formation of series of expansion fan) and then become constant and then again decreases. However, when the semi cone angle ϕ_1 = 5^o, 20^o& 40^o the above phenomena are not happening and pressure coefficient of second part cone approximately same along the position. The differences in the characteristic may be due to the bow shock developed at ϕ_1=60^o and attached shock is formed at ϕ_1 = 5^o, 20^o, 40^o.

8.3 Variation of Pressure and Total Drag Coefficient along the Cone Surface for Different Semi-Cone Angles

The variation of pressure and drag coefficient with position along the surface of bi-conic nose cone for cone base ratio 0.5 is shown in Fig.5. It can be clearly seen that the pattern of both graph is almost same. This is because total drag is summation of pressure force and viscous force and here the viscous force is very small so total drag is mainly depend on pressure force. Therefore, here all the discussion will be on pressure coefficient and in similar way, we can relate to the total drag. Now, it is noted that the pressure coefficient is increases linearly as we increase the semi cone angle but there is significant change in slope after the end of the first cone.

IX. CONCLUSIONS

A detailed numerical study of the supersonic flow past bi-conic nose cone of different configurations were conducted to understand the flow/shock features such as pressure coefficient, shock detachment distance, aerodynamic drag etc. and hence to obtain the nose cone geometry for minimum drag. The studies were conductedfor first semi-cone angles (5^o, 20^o, 40^o, 60^o)at acone base ratio (CBR) of 0.5.A total of four different nose cone geometries were investigated for drag reduction characteristics to ascertain the geometry for minimum drag.

The Mach number contours shown at different semi cone angle represents the formation of shocks such as attached as well asdetached shock features near the nose. The attached shock formsup toa semi cone angle $40^o$and there after the bow shock begins to form ahead of the nose. The current numerical simulation revealsthat the pressure coefficient decreases rapidly up to a first cone angle of 40^othereafter itshows a sudden increase

IJARSE
ISSN (O) 2319 - 8354
ISSN (P) 2319 - 8346

followed by a decreasing behaviour.The aerodynamic drag increases with increase in the first semi cone angle for a fixed cone base ratio. Thus, it may beconstruedthat the aerodynamic drag is directly proportional to the first semi cone angle, which further reveals that the minimum drag could be achieved at smaller first semi-cone angles.

REFERENCES

[1]James F.Campbell and Dorothy T. Howell, *Supersonic aerodynamics of large-angle cones,*National Aeronautics and space administration, August 1968, *NASA TN D-4719.*

[2]Bernhard H. Anderson, *Characteristic study of a bi-cone mixed compression inlet for Mach 1.8 to 2.5,* National Aeronautics and space administration, March 1969, *NASA TN D-5084.*

[3] B.E.Richards, V. Dicristina, M.L. Minges, *Heat transfer and pressure distribution on sharp and finite bluntness and bi-conic geometries at various angle of attack in Mach 15-20 flow*, September 1971.

[4]Claus Weiland, *Aero-thermodynamic data of non-winged Re-entry vehicle (RV-NV).*

LIST OF TABLE

Semi-cone angle (ϕ_1)	Shock angle obtained from current computation	Shock angle obtained theoretically by applet	% deviation in shock angle
5^o	31.02^o	30.12^o	2.98
20^o	38.92^o	37.83^o	2.88
25^o	42.80^o	42.58^o	0.5

Table 1. Comparison of obtained shock angle to the theoretical shock angle.

LIST OF FIGURES

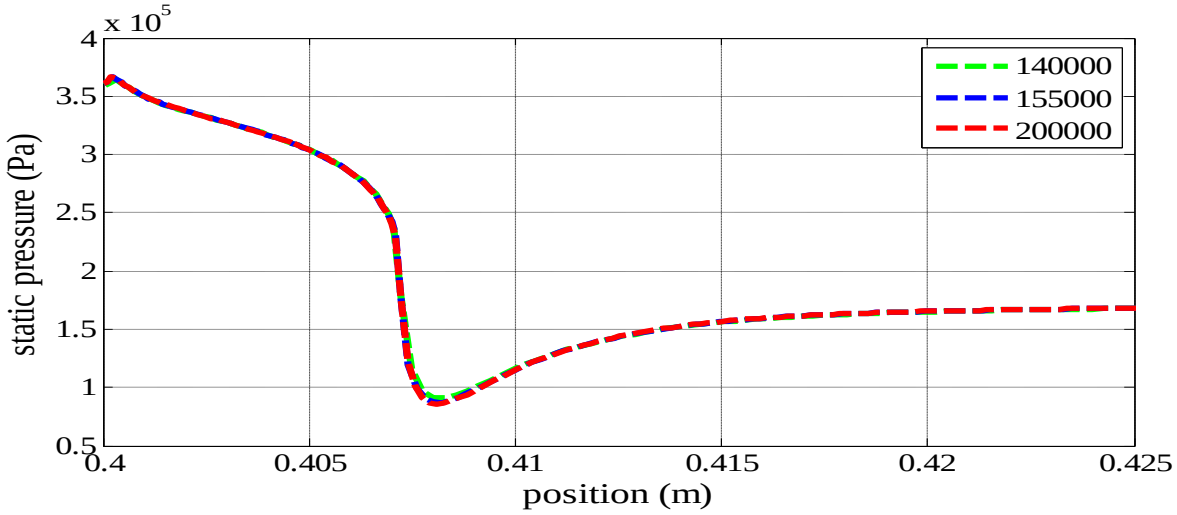

Fig. 1: variation of static pressure with positon of bi-conic noose cone at various grid point at CBR=0.5

International Journal of Advance Research in Science and Engineering
Vol. No.6, Issue No. 03 , March 2017
www.ijarse.com
IJARSE
ISSN (O) 2319 - 8354
ISSN (P) 2319 - 8346

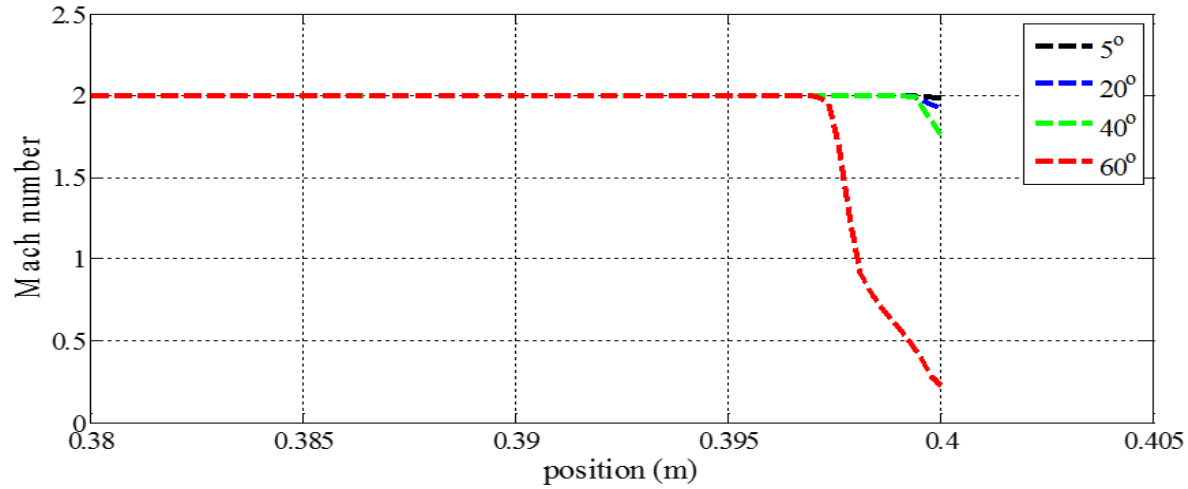

Fig. 2: variation of Mach no. with position along axis of bi-conic nose cone at CBR=0.5 and at various ϕ_1 ($\phi_1 = 2\phi_2$)

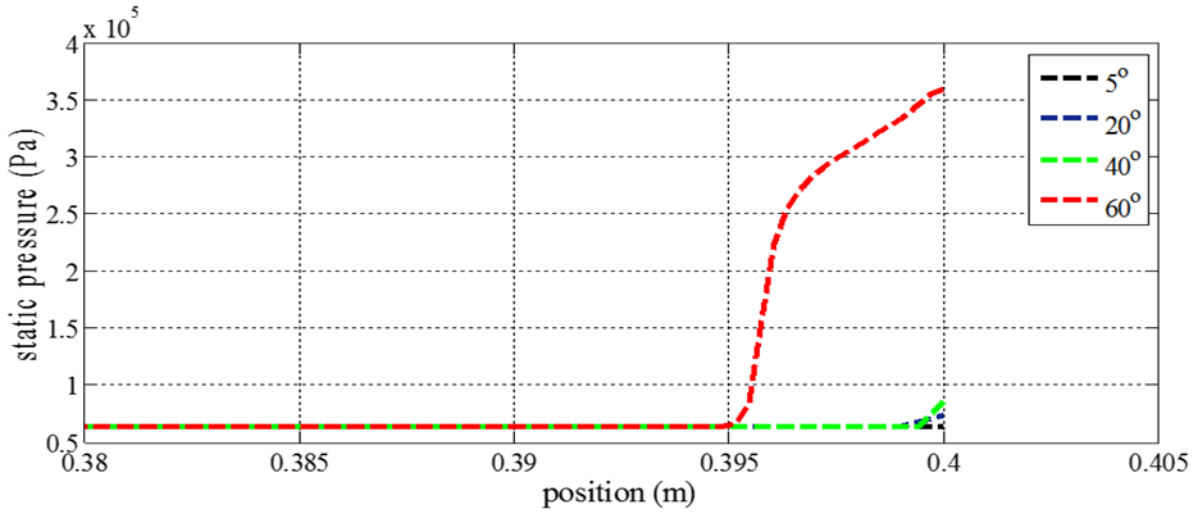

Fig. 3: variation of static pressure with position along axis of bi-conic nose cone at CBR=0.5 and at various ϕ_1 ($\phi_1 = 2\phi_2$)

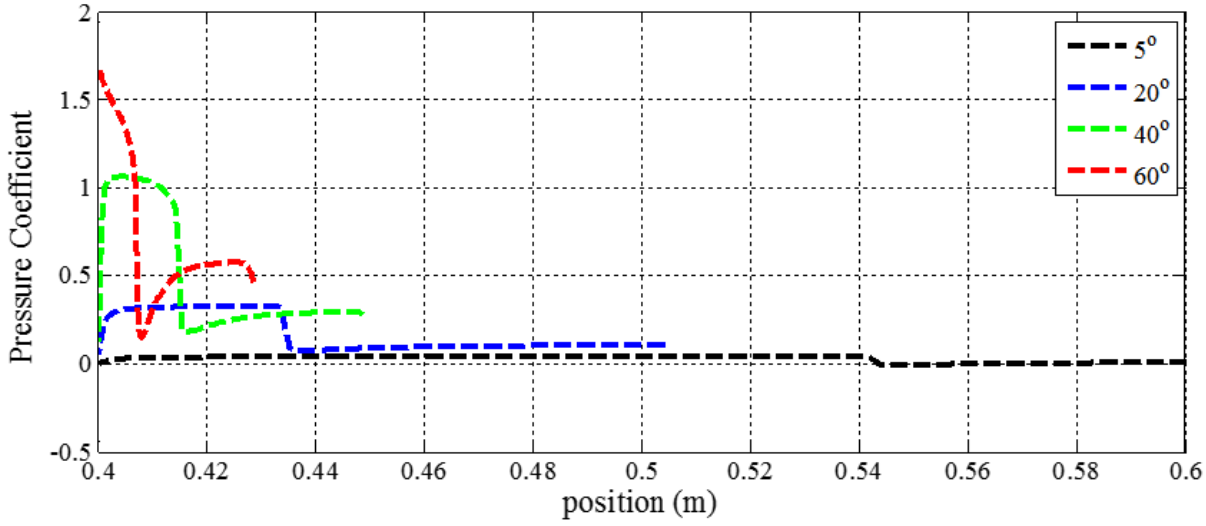

International Journal of Advance Research in Science and Engineering
Vol. No.6, Issue No. 03 , March 2017
www.ijarse.com
IJARSE
ISSN (O) 2319 - 8354
ISSN (P) 2319 - 8346

Fig. 4: variation of pressure coefficient with position along surface of bi-conic nose cone at CBR=0.5 and at various ϕ_1 ($\phi_1 = 2\phi_2$)

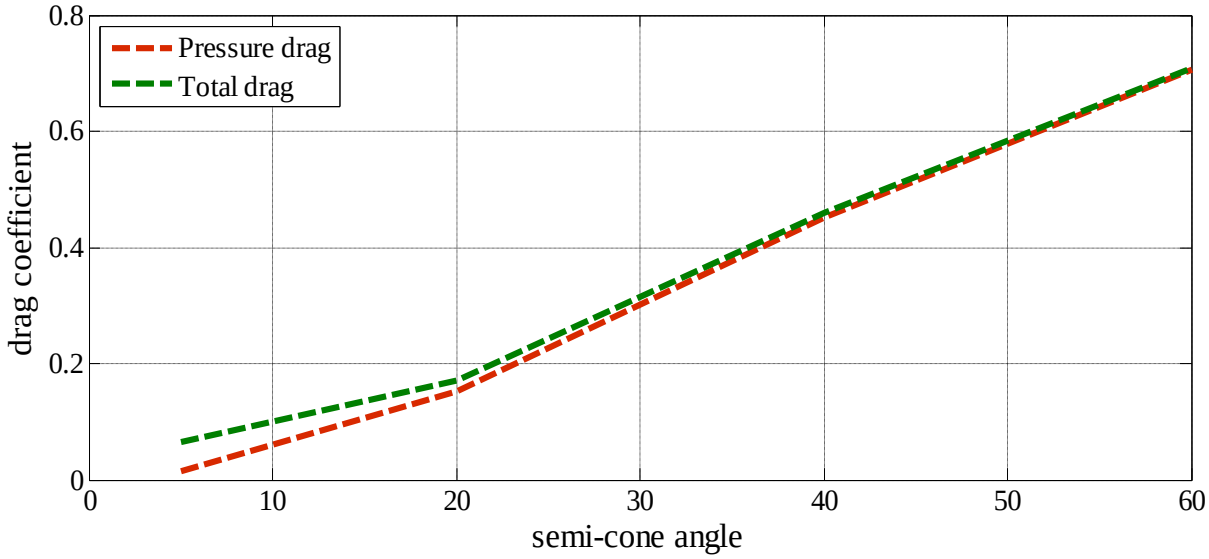

Fig. 5: Comparison of pressure & total drag coefficient at different semi cone angle at CBR=0.5